New Phytologist

Research

The desert plant *Phoenix dactylifera* closes stomata via nitrate-regulated SLAC1 anion channel

Heike M. Müller[1]*, Nadine Schäfer[1]*, Hubert Bauer[1], Dietmar Geiger[1], Silke Lautner[2], Jörg Fromm[2], Markus Riederer[3], Amauri Bueno[3], Thomas Nussbaumer[4], Klaus Mayer[4], Saleh A. Alquraishi[5], Ahmed H. Alfarhan[5], Erwin Neher[6], Khaled A. S. Al-Rasheid[1,5], Peter Ache[1] and Rainer Hedrich[1]

[1]Biocenter, Institute for Molecular Plant Physiology and Biophysics, Julius-von-Sachs-Institute, University of Wuerzburg, 97082 Wuerzburg, Germany; [2]Department of Wood Science, University Hamburg, 21031 Hamburg, Germany; [3]Biocenter, Institute for Ecophysiology and Vegetation Ecology, Julius-von-Sachs-Institute, University of Wuerzburg, 97082 Wuerzburg, Germany; [4]Plant Genome and Systems Biology, Helmholtz Center Munich, D-85764 Neuherberg, Germany; [5]College of Science, King Saud University, Riyadh 11451, Saudi Arabia; [6]Department for Membrane Biophysics, Max Planck Institute for Biophysical Chemistry, D-37077 Goettingen, Germany

Authors for correspondence:
Rainer Hedrich
Tel: +49 931 31 86100
Email: hedrich@botanik.uni-wuerzburg.de

Dietmar Geiger
Tel: +49 931 31 86105
Email: geiger@botanik.uni-wuerzburg.de

Received: *16 November 2016*
Accepted: *17 May 2017*

New Phytologist (2017)
doi: 10.1111/nph.14672

Key words: abscisic acid (ABA) signalling, cuticle, cuticular waxes, date palm *Phoenix dactylifera*, guard cells, SLAC1, S-type anion channel, stomata.

Summary

- Date palm *Phoenix dactylifera* is a desert crop well adapted to survive and produce fruits under extreme drought and heat. How are palms under such harsh environmental conditions able to limit transpirational water loss?
- Here, we analysed the cuticular waxes, stomata structure and function, and molecular biology of guard cells from *P. dactylifera*.
- To understand the stomatal response to the water stress phytohormone of the desert plant, we cloned the major elements necessary for guard cell fast abscisic acid (ABA) signalling and reconstituted this ABA signalosome in *Xenopus* oocytes. The *Phoenix* SLAC1-type anion channel is regulated by ABA kinase PdOST1. Energy-dispersive X-ray analysis (EDXA) demonstrated that date palm guard cells release chloride during stomatal closure. However, in Cl^- medium, PdOST1 did not activate the desert plant anion channel PdSLAC1 *per se*. Only when nitrate was present at the extracellular face of the anion channel did the OST1-gated PdSLAC1 open, thus enabling chloride release. In the presence of nitrate, ABA enhanced and accelerated stomatal closure.
- Our findings indicate that, in date palm, the guard cell osmotic motor driving stomatal closure uses nitrate as the signal to open the major anion channel SLAC1. This initiates guard cell depolarization and the release of anions together with potassium.

Introduction

Together, the stomata and cuticle enable plants growing in hot and dry habitats to maintain their water status. For the positive carbon gain required for growth and fruit production, a desert plant must operate stomata that retain their function during the extremely harsh summer climates of the Arabian Peninsula. Furthermore, a highly developed cuticle must cover mature leaves. Faced with heat and drought, the epidermis of desert plants with closed stomata needs to limit cuticular transpiration to extremely low values. Cuticular membranes consist of two main fractions: cutin and cuticular waxes (Holloway, 1982). Cutin is an insoluble polymer composed of hydroxy fatty acids. The cuticular waxes form the main transport barrier of the plant cuticle, reducing water loss to a minimum. The chemistry of the waterproofing waxes of desert plants should provide for the integrity of the cuticular transpiration barrier, even at elevated temperatures (Schuster *et al.*, 2016).

Guard cell potassium (K^+) ions, together with the counter anions chloride (Cl^-) and malate^{2-}, represent the major osmolytes that fuel the osmotic motor driving stomatal movements (Humble & Raschke, 1971; Hedrich, 2012 for review). In addition, nitrate also seems to play a crucial role. Nitrate is the principal nitrogen source of most plants and can accumulate to > 2% fresh weight in certain crop plants, including Gramineae. Nitrate concentrations in drought-stressed grasses are elevated (Cardenas-Navarro *et al.*, 1999). During the day, nitrate levels reach 10 mM in the cytoplasm and up to 300 mM in the vacuole (Martinoia *et al.*, 1981). The NO_3^-/H^+ exchanger CLCa is localized to the vacuole membrane and can specifically accumulate nitrate in the cell's major storage compartment (De Angeli *et al.*, 2006). Interestingly, an NTR1.1 mutant lacking the plasma membrane nitrate/H^+ co-transporter is impaired in stomatal action (Guo *et al.*, 2003). In wild-type *Arabidopsis*, alterations in nitrate metabolism feed back to guard cell slow anion currents and response to abscisic acid (ABA) (Desikan *et al.*, 2002). Slow or S-type anion currents, carried by the negative charge of chloride and nitrate, are mediated by SLAC1 and SLAH3 channels

*These authors contributed equally to this work.

expressed in the guard cells (Negi *et al.*, 2008; Vahisalu *et al.*, 2008; Geiger *et al.*, 2011; Hedrich, 2012 for review, Guzel Deger *et al.*, 2015). In *Arabidopsis*, the presence of extracellular nitrate is required to gate the anion channel (SLAH3) open. Together, these findings underlie the notion that guard cell nitrate availability is crucial for stomatal function.

Stomatal movement is controlled by guard cell turgor changes in response to partial CO_2 pressure and relative air humidity (Ache *et al.*, 2010; Bauer *et al.*, 2013). An increase in the CO_2 concentration in the substomatal cavity during daylight indicates that there is no net carbon photosynthetic gain and thus stomata close to prevent water loss. Elevated CO_2-induced responses of guard cell action require ABA and ABA signalling (Chater *et al.*, 2015).

Although the guard cell CO_2 sensory transduction is not yet fully understood, in the dicot *Arabidopsis thaliana*, major components of the signalling pathway have been identified over the years (Engineer *et al.*, 2016). By screening for CO_2-insensitive stomatal closure in *Arabidopsis*, the anion channel SLAC1 was identified (Negi *et al.*, 2008; Vahisalu *et al.*, 2008). The requirement of SLAC1 for CO_2 and ABA-induced stomatal closure has been confirmed in the monocot *Oryza sativa* (Kusumi *et al.*, 2012; Sun *et al.*, 2016). Both at high CO_2 and low humidity, guard cell responses build on ABA signalling (Bauer *et al.*, 2013; Chater *et al.*, 2015). Under dry air conditions, guard cells produce ABA autonomously and ABA binds to its RCAR/PYR/PYL-type receptor (Ma *et al.*, 2009; Park *et al.*, 2009). This ABA receptor forms a complex with the PP2C protein phosphatases ABI1, ABI2 and HAB1 and controls the activity of the kinase OST1 (Fujii *et al.*, 2009; Geiger *et al.*, 2009; Hua *et al.*, 2012; Soon *et al.*, 2012). On ABA binding to the receptor, PP2Cs become inactive (Ma *et al.*, 2009). In turn, OST1 is autophosphorylated and trans-phosphorylates the plasma membrane anion channel SLAC1 (Geiger *et al.*, 2009). Activation by phosphorylation gates SLAC1 open, anions are released and the membrane potential depolarizes. Consequently, depolarization-activated potassium channels open (Ache *et al.*, 2000). Potassium and anion loss reduces the guard cell osmotic pressure and turgor, and the stomata close.

Here, we analysed: (1) the qualitative and quantitative composition of the cuticular waxes, (2) stomata structure and function, and (3) the molecular biology of guard cells from *Phoenix dactylifera*, a non-succulent, woody hot-desert crop widespread in the deserts of the Arabian Peninsula.

Materials and Methods

Plant material and growth conditions

Two-year-old date palm (*Phoenix dactylifera*) seedlings were purchased from a commercial supplier ('Der Palmenmann', Bottrop, Germany) and cultivated at 22°C : 16°C and 50 ± 5% relative humidity (RH), day : night under a 12-h light regime at 400 μmol m^{-2} s^{-1} white light (Philips Master T Green Powers, 400 W, Amsterdam, the Netherlands). *Arabidopsis thaliana* wild-type (Col-0) plants were grown on soil in a growth chamber at 12 h : 12 h, day : night regime and 22°C : 16°C, day : night temperature for 6–8 wk at a light intensity of 120 μmol m^{-2} s^{-1} and 50 ± 5% RH.

Scanning electron microscopy (SEM)

Small pieces (2–3 mm) of fully developed (hard) pinnae were directly sputter coated with 10–15-nm gold/palladium (sputter coater BAL-TEC SCD 005) and analysed with SEM (JEOL JEM-7500F) using the detectors for secondary electrons (LEI and SEI detectors) at 5 kV. All photographs were taken from the leaf lower epidermis. Soft young pinna samples were fixed for 12–48 h at 4°C with 6.25% glutaraldehyde (Merck, Darmstadt, Germany), 50 mM Soerensen phosphate buffer, pH 7.4. The tissue pieces were then washed three times with 66 mM Soerensen phosphate buffer, pH 7.4. Samples were stepwise dehydrated with acetone, critical point dried (critical point dryer: BAL-TEC CPD 030) and metal coated as above.

Energy-dispersive X-ray analysis (EDXA)

Single, fully developed pinnae from intact leaves were darkened. The following day, pinnae were placed in a gas exchange cuvette, pre-incubated in the dark for 1 h with 400 ppm CO_2 and then kept for 1 h in the light at 1250 μmol m^{-2} s^{-1}. To fully open stomata, one group was then exposed to CO_2-free air for an additional 2 h in the light. For complete stomatal closure, another group was darkened and treated with 1000 ppm CO_2.

Leaves with open or closed stomata were immediately frozen in liquid nitrogen. After the freeze-drying process, leaves were coated with carbon before being examined by a scanning electron microscope (SEM, S-520 Hitachi, Tokyo, Japan) equipped with an energy-dispersive X-ray device (EDX Eumex Si(Li)-detector; Eumex GV, Mainz, Germany). Single-point measurements on guard cells were performed at 10 keV excitation energy, which excites a measurement area of < 2 μm in diameter. The element concentration provided by the analysis data represents the atomic ratio of the analysed ions in per cent.

Wax analysis

The analysis of the chemical composition of cuticular waxes was carried out using GC-FID (gas chromatograph with a flame ionization detector) and gas chromatography combined with mass spectrometry (GC-MS).

The protocol for extracting plant cuticular waxes has been published previously in detail by Zabka *et al.* (2008). Small adaptations were made to adjust the technique to the special features of the selected species as follows. Total leaf cuticular wax extracts of *P. dactylifera* were obtained by twice dipping entire leaflets (apart from the cut edges) for 7.5 min in 25 ml chloroform at room temperature. A precisely known amount of n-tetracosane (10 μl) was added to all extracts as an internal standard. The solvent was removed under a gentle stream of nitrogen.

The protocol for GC has been described previously by Dragota & Riederer (2007). Before GC analysis, hydroxyl-containing

compounds were transformed into the corresponding trimethylsilyl derivatives by reaction with bis-*N,O*-trimethylsilyltrifluoroacetamide in pyridine (30 min at 70°C). GC analysis was carried out using a gas chromatograph (equipped with a FID and a pressure-programmable on-column injector. Wax constituents were separated on a fused silica column DB-1 (length, 30 m; diameter, 320 μm; film thickness, 0.1 μm). The following chromatographic conditions were used: temperature programme – injection at 50°C and held for 2 min at 50°C, increased by 10°C min^{-1} to 220°C, increased by 1°C min^{-1} to 240°C, increased by 10°C min^{-1} to 320°C and held for 15 min at 320°C. Pressure programme (inlet pressure of the hydrogen carrier gas) – injection at 50 kPa and held for 5 min at 50 kPa, increased by 3 kPa min^{-1} to 150 kPa and held for 40 min at 150 kPa. Wax components were identified by GC–MS using the same chromatographic conditions as described above, but employing helium instead of hydrogen as the carrier gas. For the calculation of area-based wax contents, the total leaf surface area was used.

Transmission electron microscopy (TEM)

Intact leaves were fixed with 2% glutaraldehyde in cacodylate buffer (75 mM, pH 7.0) for 24 h (after 1 h in the fixative they were cut into small sections with a razor blade) and post-fixed with 1% osmium tetroxide at 4°C overnight. The samples were dehydrated through a series of graded acetone concentrations, 30–100%, and finally embedded in plastic according to Spurr (1964). Ultrathin sections were obtained with a ultramicrotome (Ultracut E; Leica-Reichert-Jung, Nußloch, Germany), transferred onto copper grids coated with Mowital and stained with uranyl acetate followed by lead citrate (Reynolds, 1963). Sections were viewed with a LEO 906 E TEM (LEO, Oberkochen, Germany) at 100 kV, equipped with a MultiScan CCD Camera (Model 794) from Gatan (Munich, Germany), using DIGITAL MICROGRAPH 3.3 software from Gatan to acquire, visualize, analyse and process image data.

Gas exchange measurements

Gas exchange measurements were performed using detached pinnae of at least 2-yr-old *Phoenix dactylifera spec.* plants and detached leaves of 5–6-wk-old *A. thaliana* wild-type (Col-0) plants. The leaves were cut under water to avoid xylem embolism and the petiole was immediately placed in deionized water and kept there for the whole measurement period.

Water vapour was recorded using a custom-made setup with two parallel water-cooled cuvettes with a gas stream of 1 l min^{-1}. The gas composition was adjusted and controlled by mass flow meters (red-y smart series; www.voegtlin.com) as described previously (Bauer *et al.*, 2013), and adjusted to 52.5% RH at 20°C and 380–400 ppm CO_2. Leaves were illuminated by two LEDs, which allowed illumination at different photon flux densities (Cree XLamp CXA 2530 LED for light intensities higher than 1000 μmol m^{-2} s^{-1} and Cree Xlamp CXA2520 LED for light intensities below 1000 μmol m^{-2} s^{-1}). The light beams were directed to the cuvettes via two fibre-optics (Fiber Illuminator FL-460; www.walz.com). Recordings were performed with two infrared gas analysers (LI 7000; Li-Cor, Lincoln, NE, USA).

The effect of ABA application with or without KNO_3 or KCl on transpirational water loss was measured at a photon flux density of 125 μmol m^{-2} s^{-1} for *Arabidopsis* leaves and a photon flux density of 1000 μmol m^{-2} s^{-1} for date palm pinnae. After stabilization of the transpirational water loss, ABA (final concentration, 25 μM) was fed solely or together with KNO_3 or KCl (final concentration, 5 mM) into the water reservoir.

The light dependence of transpirational water loss was measured under constant conditions of air humidity and temperature, but with different photon flux densities (0–1250 μmol m^{-2} s^{-1}) to measure different light responses.

RNA sequencing

For ABA treatment, single cut pinnae were treated for 2 h with CO_2-free air in darkness to fully open stomata, and then illuminated for 4 h at a photon flux rate of 620 μmol m^{-2} s^{-1}. Following this pre-incubation, 25 μM ABA was fed via the petiole. After 2 h, RNA was extracted from the pinnae. Controls were treated equally with ABA-free solution. RNA from leaves or single pinnae was extracted and cDNA was prepared as described previously (Bemm *et al.*, 2016).

Library preparation and RNAseq were carried out according to the *NEBNext Ultra™ RNA Library Prep* protocol (New England Biolabs, Ipswich, MA, USA), the *Illumina HiSeq 1000 System User Guide* (Illumina, Inc., San Diego, CA, USA) and the *KAPA Library Quantification Kit – Illumina/ABI Prism User Guide* (Kapa Biosystems Inc., Woburn, MA, USA). In brief, 500 ng of total RNA were used to purify poly-A containing mRNA molecules, employing the *NEBNext Poly(A) mRNA Magnetic Isolation Module*. Next, the mRNA was reverse transcribed into first-strand cDNA using reverse transcriptase and random primers, followed by second-strand cDNA synthesis. Subsequently, the resulting cDNA fragments went through an end repair process, the addition of a single 'A' base, the ligation of the barcode-containing adapters (*NEBNext Multiplex Oligos*, New England Biolabs) and a purification step. Finally, the DNA libraries were amplified by PCR. The libraries were quantified using the *KAPA SYBR FAST ABI Prism Library Quantification Kit*. Equimolar amounts were pooled, and the pools were used for cluster generation on the cBot (*TruSeq PE Cluster Kit v3*). A 2 × 100 paired-end sequencing run was performed on a HiSeq 1000 instrument, using TruSeq SBS v3 Reagents. Image analysis and base calling resulted in .bcl files, which were converted into .fastq files with CASAVA 1.8.2 software. Library preparation and sequencing were performed at the Genomics Core Facility 'KFB – Center of Excellence for Fluorescent Bioanalytics' (University of Regensburg, Regensburg, Germany; www.kfb-regensburg.de).

Data analysis

RNAseq data were mapped to the assembly of date palm (*P. dactylifera* cultivar Khalas; *Arabidopsis* Genome Initiative,

2000) with the help of TOPHAT (Trapnell *et al.*, 2012). Next, reads were summarized per gene model ($N = 37\,482$) and normalized with CUFFDIFF (Trapnell *et al.*, 2012). The normalized expression counts per genes (obtained from http://pgsb.helmholtz-muenchen.de/plant/pdact/searchjsp/index.jsp) were used to calculate differentially expressed genes from ABA-treated and control leaves (see above in the section 'Gas exchange measurements'). Genes were considered to be differentially expressed when the adjusted *P*-value was below 0.05. Best matches to *A. thaliana* TAIR10 (Arabidopsis Genome Initiative, 2000) were computed with BLASTP (Altschul *et al.*, 1990) requiring at least 30% sequence identity and a 30-amino-acid match length and by taking the match with highest bit score. For detailed analyses of the ABA experiment, only transcripts with > 10 counts in at least one treatment or control were defined as expressed and evaluated further. RNAseq data were submitted to EMBL-EBI-Annotate (https://www.ebi.ac.uk/fg/annotare/login/). ArrayExpress accession number: E-MTAB-5261.

Cloning and cRNA generation

cDNA sequences were derived from RNA-sequencing experiments (see earlier). The cDNAs of *PdSLAC1* and *PdOST1* were cloned into oocyte expression vectors (based on pGEM vectors) using an advanced uracil-excision-based cloning technique, as described previously (Nour-Eldin *et al.*, 2006). For functional analysis, cRNA was prepared using the mMessage mMachine T7 Transcription Kit (Ambion, Austin, TX, USA). Oocyte preparation and cRNA injection were performed as described previously (Becker *et al.*, 1996). For oocyte electrophysiological experiments, 10 ng of PdSLAC1 and PdOST1 cRNA were injected.

Oocyte recordings

In double-electrode voltage clamp (DEVC) studies, oocytes were perfused with Tris/Mes buffers. The standard solution contained 10 mM Tris/Mes pH 5.6, 1 mM Ca-gluconate$_2$, 1 mM Mg-gluconate$_2$, 100 mM $NaNO_3$ and 1 mM $LaCl_3$. To balance the ionic strength, the nitrate or Cl^- variations were compensated by gluconate. Solutions for selectivity measurements comprised 50 mM Cl^-, HCO_3^-, SO_4^{2-}, NO_3^-, gluconate$^-$, iodide, bromide or malate$^-$ sodium salts, 1 mM Ca-gluconate$_2$, 1 mM Mg-gluconate$_2$ and 10 mM Tris/Mes to pH 5.6. Osmolality was adjusted to 220 mOsmol kg^{-1} with D-sorbitol when appropriate. Starting from a holding potential (V_H) of 0 mV, single-voltage pulses were applied in 20-mV decrements from +60 to −200 mV. Steady-state currents (I_{SS}) were extracted at the end of the test pulses, which lasted 20 s. The relative open probability P_o was determined from current responses at a constant voltage pulse of −120 mV subsequent to the different test pulses. These currents were normalized to the saturation value of the calculated Boltzmann distribution. The half-maximal activation potential ($V_{½}$) and the apparent gating charge (z) were determined by fitting the experimental data points with a single Boltzmann equation. Instantaneous currents were extracted immediately after the voltage jump from the holding potential of 0 mV to 50-ms test pulses, typically ranging from +70 to −150 mV.

Accession numbers

Sequence data from this article can be found in the GenBank/EMBL databases under the following accession numbers: PdSLAC1 (XP_008780343.1); PdOST1 (XP_008792595.1).

Results

In a recent study on date palm, it was shown that heat and drought stress only slightly affect photosynthesis (Arab *et al.*, 2016). This raises the question of how the photosynthetic apparatus of the hot-desert plant is protected from heat and dehydration stress. To answer this question, we focused on the water-resistant cuticle covering the leaf and the water gates (stomata) of the date palm.

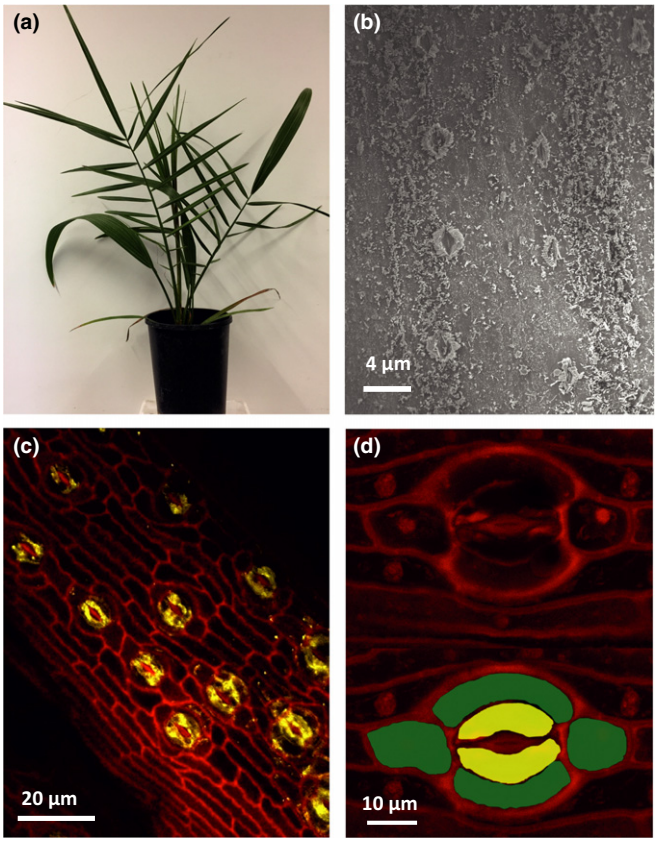

Fig. 1 Date palm (*Phoenix dactylifera*) stomata characteristics. (a) Two-year-old date palms grow three to five pinnate leaves. (b) Electron micrograph of the upper leaf surface. Stomata are arranged in rows, as in grasses. The epidermis is covered with epicuticular waxes. (c, d) Laser scanning images of the date palm leaf surface stained with propidium iodide (excitation at 458 nm, fluorescence recorded at wavelengths of 490–550 nm). (d) Stomata are surrounded by lateral and polar subsidiary cells (highlighted in green in the right image, guard cells are coloured yellow). These two pairs of cells very probably produce the waxy stomatal chimney.

Stomata are surrounded by epicuticular wax chimneys

To examine the morphology of the leaf surface of 2-yr-old palms (Fig. 1a), samples of mature pinnae were directly sputter-coated with gold/palladium and analysed by SEM. Stomata were found to be arranged in highly ordered rows along the blade of the leaflets (Fig. 1b), reminiscent of stomatal patterning in grasses. The distance between files was 66.2 ± 7 μm ($n = 15$) with 20 ± 2 stomata mm^{-1} file length ($n = 16$). In contrast with grasses, however, stomata were not dumbbell-shaped, but of the tetracytic type (Fig. 1c,d; Luis *et al.*, 2010). The size of mature closed stomata was *c.* 15.5 μm (± 1.3; $n = 16$) in length and 8.25 μm (± 0.95, $n = 16$) in width, at a density on both upper and lower leaf surfaces of 180–200 stomata mm^{-2} (Supporting Information Fig. S1a). Interestingly, the desert plant has the same stomatal density as *Arabidopsis* – a plant adapted to low light and cold (Langer *et al.*, 2004). Thus, *Phoenix* must restrict transpiration by increased closing of stomata (see later) and an efficient cuticular transpiration barrier.

We found that each stoma was surrounded by a wall of cuticular wax (Fig. 2a,b), building stomatal wax chimneys (Barthlott *et al.*, 1998). Such a ring of epicuticular wax around the stomata increases the boundary resistance for stomatal transpiration. To gain insights into the nature of cuticle wax extracts from *P. dactylifera,* leaf surfaces were obtained by chloroform extraction and samples were analysed using GC (for details, see methods of Dragota & Riederer (2007) and Zabka *et al.* (2008)). The cuticular wax coverage of fully developed leaflets from *P. dactylifera* was 26.82 ± 1.93 μg cm^{-2} (mean value ± SD, $n = 5$), mainly composed of long-chain aliphatic substances, such as *n*-alkanes, primary alcohols, fatty acids and alkyl-esters, with carbon chain lengths from 25 to 36 (*n*-alkanes), 22 to 35 (alcohols), 20 to 34 (fatty acids) and 40 to 50 (alkyl-esters). The main component was dotriacontanoic acid (C_{32}), with coverage of 5.48 ± 0.16 μg cm^{-2}. The alkyl-ester with a carbon chain length of 48 was the second most abundant substance (2.42 ± 0.83 μg cm^{-2}), followed by the primary alcohol with carbon chain length C_{32} (1.69 ± 0.30 μg cm^{-2}). Traces of pentacyclic triterpenoids were also found. The high concentration of long-chain aliphatic substances in the waxes of *P. dactylifera* suggests that the cuticular wax has a high crystallinity.

To gain further insights into the origin of the cuticular wax chimneys surrounding the guard cells, we analysed young pinnae using SEM. During fixation before SEM analysis, a series of acetone treatments was performed. The waxes were partially removed, but the remnants could be allocated to the subsidiary cells (Fig. S1b), indicating that the cuticular wax chimneys might originate from epicuticular wax production of subsidiary cells.

Guard cells have a lateral and polar pair of subsidiary cells

We largely de-waxed the leaf samples and examined the stomatal complexes using laser-scanning microscopy (LSM). After staining with propidium iodide, LSM images clearly showed that each guard cell pair is surrounded by a pair of lateral and polar subsidiary cells (Fig. 1c,d), a feature that *P. dactylifera* shares with non-grass monocots (Sack & Chen, 2009; Raissig *et al.*, 2016). To gain insights into the ultrastructure of the guard cell complex, we used TEM. Leaf sections were fixed in glutaraldehyde and osmium tetroxide buffer. Ultrathin cross-section inspection showed two smaller guard cells in complex with a pair of lateral subsidiary cells of a large size (Fig. 3a). The subsidiary cells sheathed the guard cells in a way that allowed for stomatal gas exchange between the atmosphere and the substomatal cavity, whilst preventing any physical contact of guard cells with epidermal or mesophyll cells (Fig. 3a,b). Guard cells themselves were characterized by a large vacuole and nucleus, numerous mitochondria and a few smaller

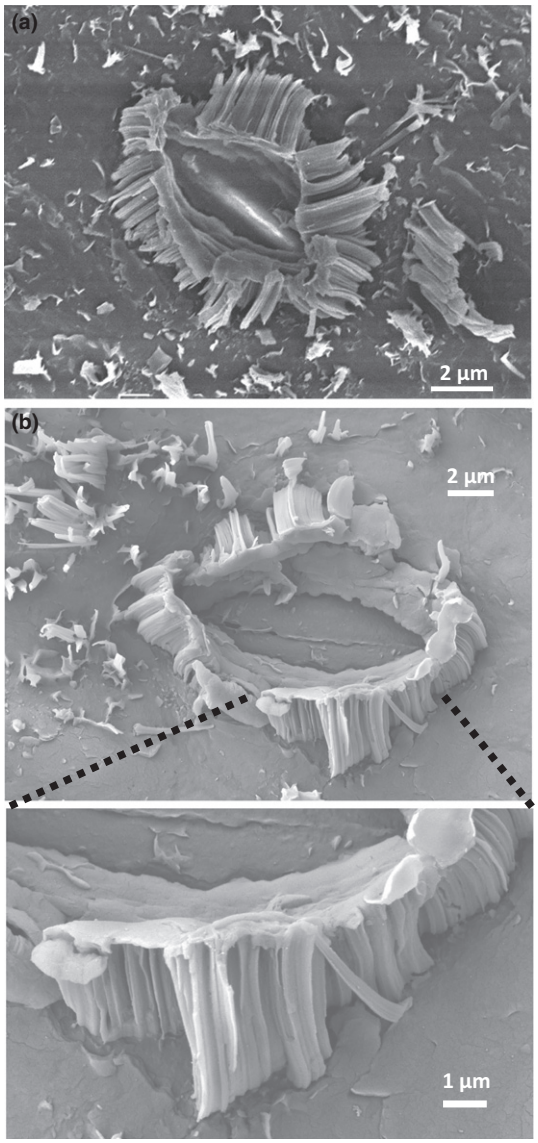

Fig. 2 Date palm (*Phoenix dactylifera*) stomata morphology. (a, b) Raster electron micrograph from a stoma on the lower leaf surface. Stomata are surrounded by a huge epicuticular wax chimney, thereby increasing the thickness of the boundary layer above the stomatal pore and, consequently, the total resistance to stomatal transpiration. The wax seems to emerge from the cells neighbouring the guard cells. (b, lower image) Magnification of a stomatal wax chimney.

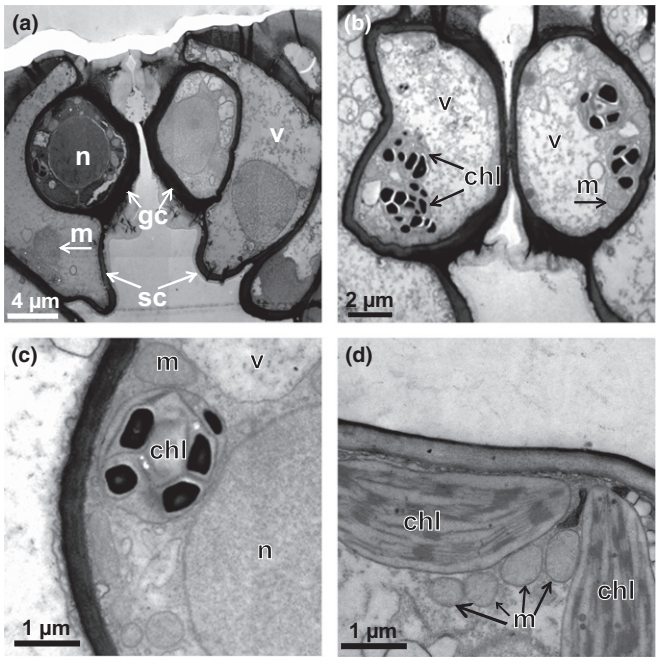

Fig. 3 Subcellular components of date palm (*Phoenix dactylifera*) stomata, transmission electron microscopy (TEM) cross-sections. (a) Overview of a stomatal complex with guard cells (gc), subsidiary cells (sc) and neighbouring epidermal cell. The pair of guard cells is clearly separated from epidermal cells by subsidiary cells. Subsidiary cells possess large central vacuoles (v) and mitochondria (m). Guard cells contain a large nucleus (n). (b) Detailed view of the guard cell pair. The guard cells do not share plasmodesmatal connections with the subsidiary cells, and so are symplastically isolated. Guard cells exhibit large vacuoles (v), numerous mitochondria (m) and few chloroplasts (chl). (c) Detailed view of a guard cell chloroplast containing massive starch grains (black spots). (d) Mesophyll cell showing large chloroplasts (chl) with stroma and grana thylakoids in close contact with numerous mitochondria (m), indicating high photosynthetic activity.

chloroplasts containing starch grains (Fig. 3c). These subsidiary cells were in contact with common epidermal and mesophyll cells. The latter were characterized by large chloroplasts (Fig. 3d). In open stomata, the thick inner cell walls of the guard cell pair appeared to be attached to each other. These guard cell features suggest that closed stomata in date palm form a tight water shield.

Stomata open at high light intensities

In the dark, respiratory CO_2 in the leaf intercellular spaces, including the substomatal cavity, is recognized by the guard cell's CO_2 sensor. This rise in CO_2 in combination with darkness arrests stomata in the closed state (Hashimoto *et al.*, 2006). When sunlight in the blue and red light spectra is detected, stomata open. Blue light with a low fluency rate is sensed by the guard cell phototropin system, which activates the plasma membrane proton pump AHA1 (Yamauchi *et al.*, 2016 and references cited therein). Consequently, proton extrusion increases, the plasma membrane hyperpolarizes and the resulting proton motive force energizes K^+ uptake (Roelfsema *et al.*, 2001), thereby driving osmotic swelling of the guard cells and stomatal opening. High-fluency red light activates photosynthetic CO_2 fixation by mesophyll cells (Roelfsema & Hedrich, 2005). The drop in CO_2 concentration in the substomatal cavity is sensed by a so far unidentified guard cell CO_2 sensor (Hashimoto *et al.*, 2006; Hu *et al.*, 2010; Tian *et al.*, 2015), anion channels are closed, blue light-induced pumps foster membrane hyperpolarization, so promoting K^+ salt uptake (Roelfsema *et al.*, 2002; Marten *et al.*, 2007).

To induce opening of *Phoenix* stomata, we applied white light of increasing fluency rates. Using dark-adapted leaves mounted

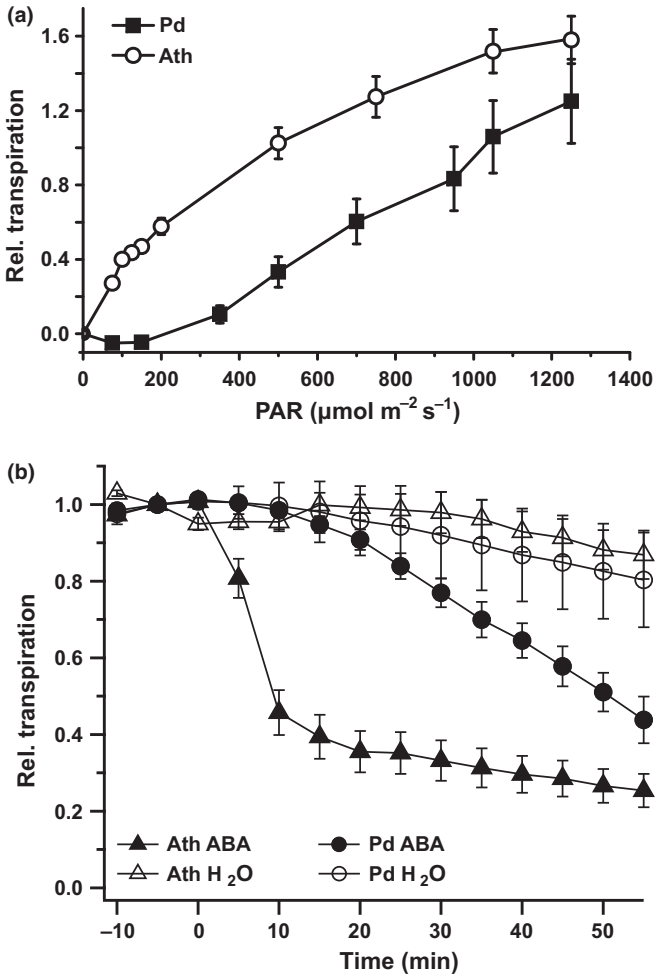

Fig. 4 Date palm (*Phoenix dactylifera*) stomata physiology measured by infrared gas exchange. The relative transpiration rate mirrors the aperture of the stomata. (a) Date palms need high light intensities for stomatal opening. *Arabidopsis thaliana* (Ath) stomata open at light intensities as low as 200 µmol m^{-2} s^{-1}, an intensity at which the desert plant *P. dactylifera* (Pd) only started to open its stomata. Even at very high intensities of > 1200 µmol m^{-2} s^{-1}, saturation was not observed in date palm. *Arabidopsis*, $n = 8 \pm$ SE; date palm, $n = 13 \pm$ SE. (b) *Phoenix dactylifera* only slowly responds to abscisic acid (ABA) application. Stomata of both plant species opened in the light (*Arabidopsis*, 125 µmol m^{-2} s^{-1}; *Phoenix*, 1000 µmol m^{-2} s^{-1}) at ambient CO_2. ABA was applied via the petiole. *Arabidopsis* leaves closed stomata 5 min after ABA application. This process was largely completed within 10 min, finishing in < 20 min ($n = 6 \pm$ SE). By contrast, date palm stomata initiated closure after 20 min. The closing process was remarkably slower compared with *Arabidopsis* and was not finished after 1 h of ABA treatment ($n = 10 \pm$ SE).

in a gas exchange chamber, we monitored water vapour emission (transpiration) by infra-red gas analysis (IRGA) at 50% RH and 400 ppm CO_2 under optimal water supply. Transpiration of date palm leaves did not increase above the dark level at fluency rates of up to 250 μmol m^{-2} s^{-1} (Fig. 4a). In this range of low light intensities, transpiration in *Arabidopsis* is already well induced and was 30% higher than the transpiration of date palm pinnae (Fig. 4a). On increasing the quantal fluxes to 300 μmol m^{-2} s^{-1} and stepwise further to 1250 μmol m^{-2} s^{-1}, transpiration of palm leaves increased in a linear fashion, whereas transpiration of *Arabidopsis* leaves tended to saturate at light intensities above 1000 μmol m^{-2} s^{-1}. At these high quantum flux rates, transpiration of *Arabidopsis* and date palm were comparably high. Nonetheless, the high-light desert plant did not show any signs of light saturation phenomena at the peak fluency rate that we could impose experimentally.

The stomatal response to external ABA is delayed

The stress hormone ABA controls the water status of a plant. When access to soil water is restricted, ABA is synthesized and directed to the guard cells to induce stomatal closure. Guard cells, however, can sense dry atmospheres directly (Bauer *et al.*, 2013). With a drop in air humidity, guard cells produce their own ABA, thus triggering closure of the water gates.

To test the ABA response of stomata in excised palm leaf pinnae, we fed this stress hormone into the transpiration stream (Fig. 4b). Following the onset of ABA feeding to pinnae with stomata pre-opened at 1000 μmol m^{-2} s^{-1}, 380 ppm CO_2 and 50% RH, transpiration slowly ceased after a delay of *c.* 20 min, but stomata did not reach steady closure within 1 h. When *Arabidopsis* leaves of about the same length were challenged with ABA, transpiration began to drop after 5 min, was halved at 10–12 min, reaching its minimum steady state after 20 min (Fig. 4b). Is this difference the result of different velocities in water ascent in the xylem of the two plants? To compare the ascent of ABA, we applied 3-(3,4-dichlorophenyl)-1,1-dimethylurea (DCMU), a blocker of chloroplast photosynthetic electron transport, and followed DCMU action by imaging with a pulse-amplitude-modulated fluorometer. The speed of DCMU-induced loss of chlorophyll fluorescence appeared even faster with *Phoenix* than with *Arabidopsis* (Fig. S2). This indicates that ABA export from the xylem, import into guard cells or ABA signal transduction (see below) in the date palm leaf is reduced.

Only a small pool of RNA is differentially expressed in response to drought and ABA

To gain insights into the ABA genes differentially expressed in response to soil drying, we performed RNAseq analysis with date palm pinnae in which ABA, as a substitute for soil drought stress, was fed into the transpiration stream. From this study, we could identify components of guard cell light, CO_2 and ABA signalling pathways (Table S1).

In the latter category, the ABA signalling pathway, we identified 153 differentially expressed genes (Table S1). When comparing ABA genes in date palm with those from the *Arabidopsis* guard cell (Bauer *et al.*, 2013), we found 46 expressed orthologues that responded to treatment with the stress hormone. These included well-known key elements of ABA signal transduction that control the transcriptional regulation of drought stress genes; for example, phosphatases from the PP2C family, ATP binding cassette (ABC) transporters, late embryogenesis abundant proteins (LEAs) and the guard cell transcription factor MYB74 (Bauer *et al.*, 2013). Interestingly, 106 genes that were differentially regulated in *Phoenix* did not respond to ABA in *Arabidopsis*. This behaviour indicates that both plants operate the same basic ABA signalling elements, but, at the same time, also engage additional, individual response schemata.

Stomatal closure is based on OST1 activation of SLAC1

In addition to the transcriptional regulation of ABA genes, as required for long-term stress adaptation, guard cells also respond to sudden challenges in water homeostasis by fast stomatal closure. This process is based on guard cell ion release, with a consequent reduction in cell volume and turgor (Hetherington & Woodward, 2003). The key player in membrane ion release in guard cells is the anion channel SLAC1 (Negi *et al.*, 2008; Vahisalu *et al.*, 2008). In *Arabidopsis*, this anion channel type is activated by the core ABA signalosome via the PYR/ABI1/OST1 triad (Soon *et al.*, 2012). When ABA binds to its receptor from the PYR/PYL family, the PP2C protein phosphatases, such as ABI1, ABI2 or HAB1, are inactivated and, in turn, the SnRK2 protein kinase OST1 starts to operate (Fujii *et al.*, 2009; Geiger *et al.*, 2009; Ma *et al.*, 2009; Park *et al.*, 2009; Hua *et al.*, 2012). When derepressed from ABI1 de-phosphorylation, OST1 auto-phosphorylates and trans-phosphorylates its target protein, SLAC1 (Geiger *et al.*, 2009; Lee *et al.*, 2009).

To test whether the fast ABA signalling pathway initiates a similar anion channel opening mechanism in date palm guard cells, we cloned the *Phoenix* PdSLAC1 and PdOST1. Phylogenetic analysis revealed that PdSLAC1, just like OsSLAC1, clearly groups into the SLAC1 subgroup of the SLAC/SLAH anion channel family (Fig. S3a). Likewise, PdOST1 groups together with ABA-dependent SnRK2 kinases, such as AtOST1 (Fig. S3b), confirming that both *P. dactylifera* proteins are closely related to known ABA signalling components from, for example, *Arabidopsis*. Following reconstitution in *Xenopus laevis* oocytes, we functionally characterized the electric properties and the regulation of the putative anion channel PdSLAC1. To assess the regulation of PdSLAC1 by SnRK2 kinase OST1, we monitored the activity of the channel in the presence and absence of *Phoenix* OST1 in oocytes with the DEVC technique (cf. Geiger *et al.*, 2009; Lee *et al.*, 2009). However, we could not detect anion currents in oocytes injected with PdSLAC1 alone (Fig. 5a). Co-expression of SLAC1 with PdOST1 did not result in S(slow)-type anion currents in chloride-based solutions, but such currents could be detected in nitrate-based medium (Fig. 5a). Indeed, in 10 mM external NO_3^-, 20-s voltage pulses elicited macroscopic SLAC1 currents that deactivated at negative membrane potentials

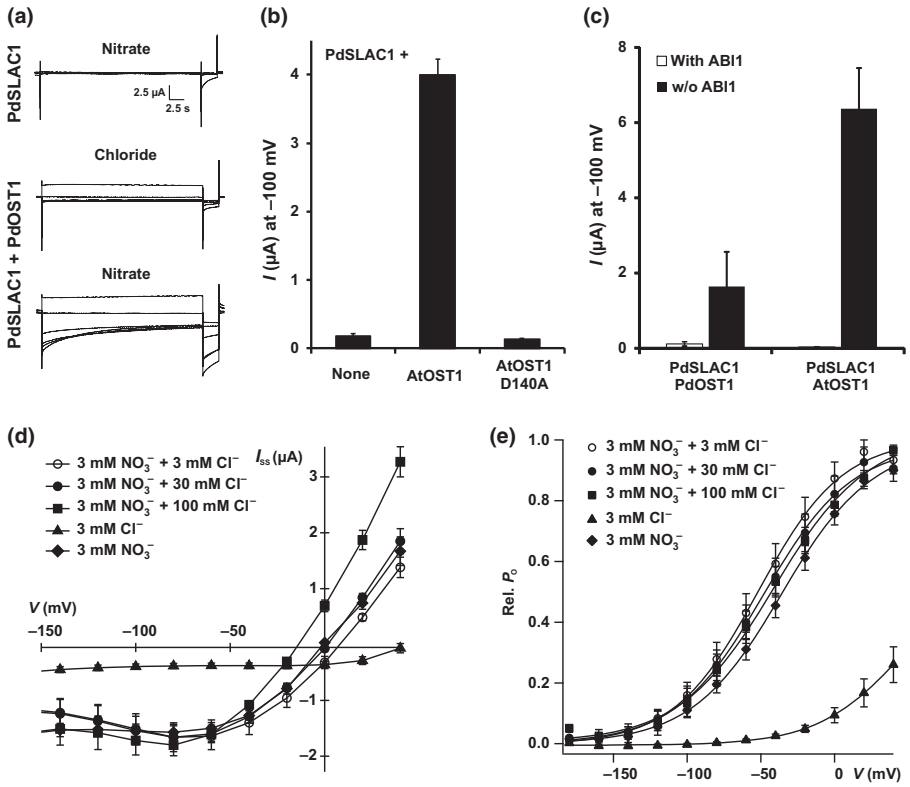

Fig. 5 PdSLAC1 is activated by PdOST1 and preferentially mediates nitrate currents. (a) Whole-oocyte currents of oocytes expressing PdSLAC1 or co-expressing PdSLAC1 and PdOST1 in medium containing either 10 mM chloride or nitrate. The experiment was performed with the standard voltage protocol. Representative cells are shown. (b) On co-expression of PdSLAC1 with AtOST1, macroscopic anion currents could be monitored in nitrate-based medium. The kinase dead mutant of OST1 (D140A) was, however, not capable of activating PdSLAC1. Instantaneous currents recorded at −100 mV in the presence of 100 mM NO_3^- are shown ($n = 7$ experiments, mean ± SE). (c) Instantaneous currents of PdSLAC1-injected oocytes recorded at −100 mV co-expressing different combinations of PdSLAC1, At- or PdOST1 and AtABI1. Pd- or AtOST1-induced PdSLAC1 currents were significantly reduced by ABI1 co-expression in the presence of 100 mM NO_3^- ($n \geq 6$ experiments, mean ± SE). (d) NO_3^- and voltage dependence of steady-state currents (I_{SS}) from PdSLAC1- and PdOST1-co-expressing oocytes. With 3 mM NO_3^- in the bath medium, PdSLAC1-mediated currents could be observed. The addition of up to 100 mM Cl^- in the bath medium in the presence of 3 mM NO_3^- shifted the reversal potential (V_{rev}) to negative voltages relative to the situation with 3 mM NO_3^- alone or 3 mM Cl^- ($n = 9$, mean ± SE). (e) Relative voltage-dependent open probabilities (Rel. P_o) of PdSLAC1- and PdOST1-mediated currents under the conditions used in (c). Data points were fitted with a Boltzmann equation (continuous line; $n = 5$, mean ± SE).

(Fig. 5a). These slow deactivation characteristics are reminiscent of S-type anion currents in *Arabidopsis* guard cells monitored in their natural environment (Guzel Deger *et al.*, 2015) and following the expression of AtSLAC1 injected into *Xenopus* oocytes (Geiger *et al.*, 2009).

Because ABI1 in *Arabidopsis* guard cells inhibits responses to nitrate (Desikan *et al.*, 2002), as well as AtOST1 activation of AtSLAC1 (Geiger *et al.*, 2009; Maierhofer *et al.*, 2014a), we co-expressed *Phoenix* PdSLAC1, together with either PdOST1, AtOST1 or the kinase inactive mutant D140A of AtOST1. Although both wild-type (WT) kinases were capable of activating PdSLAC1, the kinase dead mutant was not (Fig. 5b,c). This indicates that phosphorylation of PdSLAC1 is necessary for anion channel activation (cf. Geiger *et al.*, 2009). On co-expression of WT OST1 kinases and PdSLAC1 with ABI1, we found that PdSLAC1-mediated anion currents were abolished, irrespective of the origin of the activating kinase (Fig. 5c). These findings indicate that the core of the fast ABA signalling pathway is conserved between guard cells of the dicot *Arabidopsis* and the desert monocot *Phoenix*.

PdSLAC1 is activated by nitrate

Above, we documented that, in contrast with AtSLAC1, PdSLAC1 mediates macroscopic anion currents in the presence of nitrate alone. Of note is that this behaviour is also known from the SLAC1 homologue AtSLAH3 (Geiger *et al.*, 2011). We therefore examined the nature of the SLAH3-type nitrate dependence of PdSLAC1 using buffers containing different chloride to nitrate ratios (Fig. 5d). Anion currents recorded in the presence of 3 mM extracellular chloride were very weak compared with 3 mM nitrate (Fig. 5d). This corresponds to the observation that PdSLAC1 is a preferentially NO_3^--permeable channel with a 20 times higher permeability to NO_3^- than Cl^- (Fig. S4). However, in the presence of 3 mM nitrate and when the chloride concentration was increased from 3 to 30 and 100 mM, the reversal potential shifted to negative membrane potentials (Fig. 5d). By analysing the relative open probability of PdSLAC1, we observed a shift in the voltage-dependent gating properties of the anion channel towards negative membrane potentials only in response to nitrate, but not to chloride, application (Fig. 5e). This

behaviour indicates that nitrate modifies the PdSLAC1 gate for chloride permeation.

To further substantiate the effect of nitrate on the voltage-dependent gating of PdSLAC1, we determined the relative open probability as a function of the external nitrate concentration. When exposed to increasing external nitrate concentrations ($[NO_3^-]$), the peak efflux currents and the relative open probability shifted towards negative membrane potentials (Fig. 6a,b). This PdSLAC1 response indicates that, under a physiological $[NO_3^-]$ of 2–5 mM (Speer & Kaiser, 1991), nitrate is not only conducted by the channel, but can also increase the activity of PdSLAC1. In other words, nitrate gates PdSLAC1 open, increases the plasma membrane anion conductance (both for nitrate and chloride) of guard cells and induces stomatal closure.

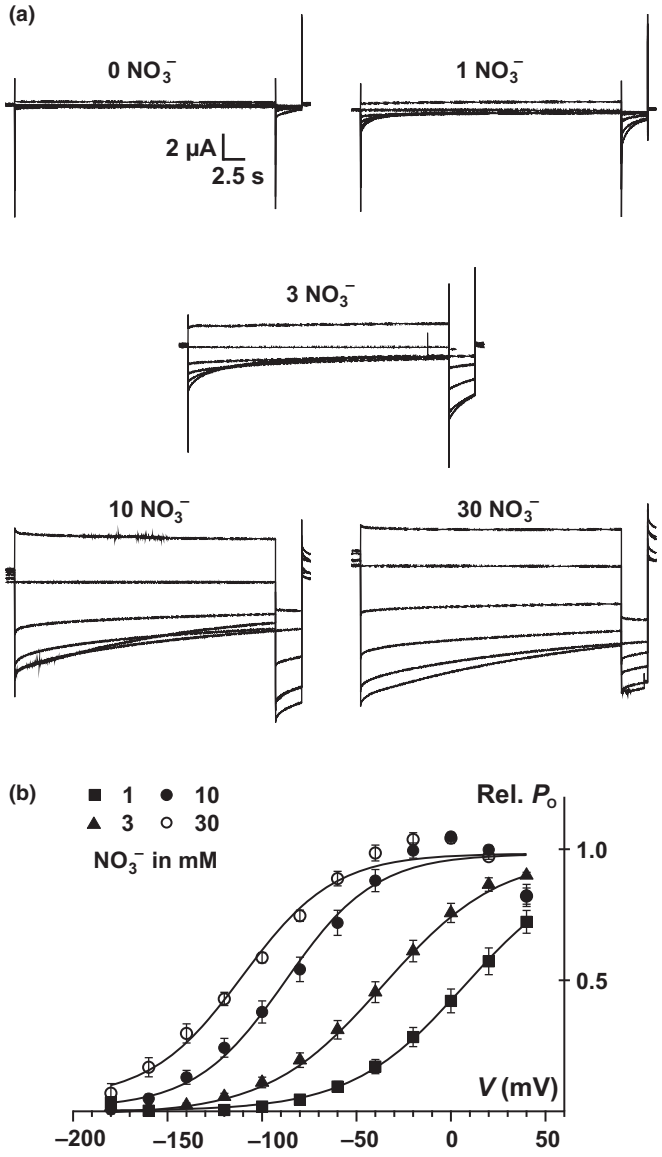

Fig. 6 Nitrate gates PdSLAC1 open. (a) Whole-oocyte currents of PdSLAC1- and PdOST1-co-expressing *Xenopus* oocytes recorded in the presence of different nitrate concentrations (as indicated). Voltage pulses lasting 20 s were applied, ranging from +40 to −180 mV in 20-mV decrements, followed by a 3-s voltage pulse to −120 mV. The holding potential was clamped to 0 mV. (b) The relative open probability (Rel. P_o) of PdSLAC1- and PdOST1-expressing oocytes at the indicated NO_3^- concentrations as a function of the membrane potential. Data points were fitted with a single Boltzmann equation (solid lines, $n \geq 9$ experiments, mean ± SE).

Petiole-fed nitrate accelerates ABA-dependent stomatal closure

The heterologous expression and functional analysis of major components of the fast ABA signalling pathway in oocytes demonstrated that the desert plant is well equipped with ABA signalling machinery that enables a quick response to drought, provoking stomatal closure. In contrast with *Arabidopsis* stomata, however, initial gas exchange measurements with date palm pinnae revealed only slow and incomplete stomatal closure in response to petiole-fed ABA (Fig. 4b). A remarkable difference between *Arabidopsis* SLAC1 and its counterpart from *P. dactylifera* is substantiated by the nitrate-dependent opening of the date palm anion channel, whereas AtSLAC1 opens without the need for extracellular nitrate. To prove that extracellular nitrate accelerates stomatal closure *in planta*, we monitored ABA-dependent stomatal closure of date palm or *Arabidopsis* leaves via transpiration measurements in the presence of either 5 mM KCl or KNO_3. Indeed, on feeding ABA diluted in a KNO_3 solution, stomatal closure of date palm pinnae was markedly accelerated and saturated after 30 min (Fig. 7a), whereas the response of *Arabidopsis* leaves appeared to be unchanged or even slowed (Fig. 7b). The application of KCl + ABA instead of KNO_3 did not significantly accelerate stomatal closure in date palm or in *Arabidopsis* leaves (Fig. S5a, b). The treatment with KNO_3 or KCl without ABA did not induce stomatal closure in either *Arabidopsis* or *Phoenix* leaves (Figs 7a,b and S5a,b).

Stomatal closure is associated with the release of osmotically active chloride anions

PdSLAC1, just like *Arabidopsis* SLAH3, but in contrast with AtSLAC1, opens only when nitrate is present at the extracellular side of the membrane. When activated, PdSLAC1 mediates both nitrate and chloride release (Fig. 5d). However, the date palm anion channel prefers nitrate to chloride with a P_{NO3}/P_{Cl} ratio of 20 (Fig. S4). Thus, one might ask whether date palms release nitrate as the main osmotically active anion as opposed to releasing chloride. To answer this question, we compared the Cl, S and P contents of fully opened and closed guard cells of mature date palm pinnae using EDXA (Fig. 7c,d). Although the sulphur and phosphorus contents did not change markedly (Fig. 7d), Cl was 70% lower in closed relative to open stomata (Fig. 7c). Although nitrogen changes cannot be determined by EDXA experiments, the dramatic decrease in chloride in closed guard cells indicates that, in date palms, it is mainly chloride anions that are released during stomatal closure, just as in the moncot maize (Raschke & Fellows, 1971).

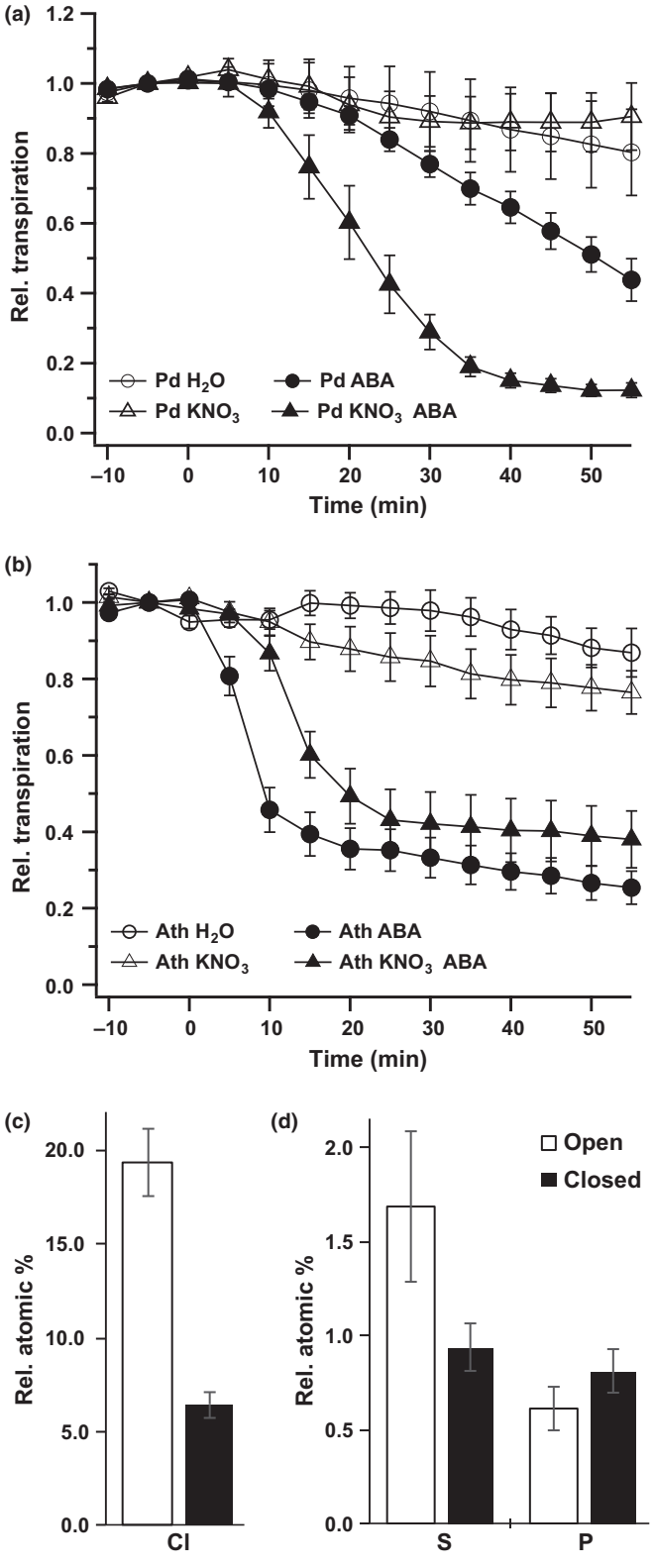

Fig. 7 Nitrate accelerates abscisic acid (ABA)-dependent stomatal closure. (a) Infrared gas exchange experiments revealed that date palm (*Phoenix dactylifera*) stomata close more rapidly and more completely in the presence of ABA and nitrate (5 mM) ($n \geq 8$ experiments, mean ± SE). (b) ABA-dependent stomatal closure of *Arabidopsis* leaves was not markedly modified in the presence of 5 mM nitrate ($n \geq 5$ experiments, mean ± SE). (c, d) Energy-dispersive X-ray analysis (EDXA) experiments with fully closed or opened date palm guard cells were performed to determine relative element changes ($n \geq 6$ experiments, mean ± SE). (c) Closed date palm guard cells exhibited 70% less Cl than guard cells of fully opened stomatal complexes ($n = 6$ experiments, mean ± SE). (d) Sulphur (S) and phosphorus (P) contents in guard cells of date palms did not display major changes ($n \geq 6$ experiments, mean ± SE).

Discussion

The palms are members of the monocot plant group together with grasses. Although stomatal development and density have been studied mainly in the dicot *Arabidopsis*, major master transcriptional regulators of stomatal initiation have also been found to be conserved in grasses (Caine *et al.*, 2016). Stomata of the basal monocot *Phoenix* and other non-grass monocots have kidney-shaped guard cells (Fig. 1c,d, c.f. Stebbins & Khush, 1961), whereas grasses develop dumbbell-shaped sphincters.

SLAC1 is the key for ABA-dependent stomatal closure

Most guard cell anion channel investigations have been conducted on dicots. S-type and R-type anion currents were first identified in *Vica faba* (Schroeder & Hagiwara, 1990; Hedrich, 2012; Roelfsema *et al.*, 2012 for review). In such faba bean studies, ABA was shown to control S-type and R-type channels (Levchenko *et al.*, 2005). Later, the molecular nature of the channels behind the distinct types of currents was identified in the model dicot *Arabidopsis* (Negi *et al.*, 2008; Vahisalu *et al.*, 2008; Meyer *et al.*, 2010). In *Arabidopsis*, guard cells express and require two S-type channels: SLAC1 and SLAH3 (Geiger *et al.*, 2011; Guzel Deger *et al.*, 2015). Both anion channels are nitrate permeable, but only SLAC1 has a major conductance for chloride, even in the absence of nitrate (Geiger *et al.*, 2009). This chloride permeability is essential for the appropriate response of *Arabidopsis* guard cells to elevated CO_2 and ABA (Negi *et al.*, 2008; Vahisalu *et al.*, 2008). Only when AtSLAH3 is additionally 'over'-expressed under the AtSLAC1 promoter is this nitrate-dependent anion channel, with its relative weak chloride permeability, capable of rescuing the SLAC1 loss-of-function defect (Negi *et al.*, 2008). In addition, the *slac1-1* mutant can be rescued when SLAH1 co-expression renders SLAH3 nitrate independent and increases its chloride conductance (Cubero-Font *et al.*, 2016).

S-type currents in grasses were first recorded in *Hordeum vulgare* guard cells (Koers *et al.*, 2011) and, recently, rice OsSLAC1 expressed in the heterologous *Xenopus* oocyte expression system has been shown to mediate S-type anion currents (Sun *et al.*, 2016). The latter study also showed that the OST1 kinase is necessary for the activation of rice SLAC1, confirming earlier studies in *Arabidopsis* (Geiger *et al.*, 2009; Lee *et al.*, 2009). This indicates that, in dicots and monocots, SLAC1 is similarly regulated by ABA. In this study with *P. dactylifera* PdSLAC1, we show that the date palm anion channel requires extracellular nitrate for gate opening. When guard cells are open, PdSLAC1 prefers nitrate to chloride, but, in the presence of low

nitrate on its external side, the channel is also permeable to chloride (Fig. 5d,e).

Guard–subsidiary cell shuttle transport

As well as having stomata ordered in rows, date palm stomata, like grasses, have subsidiary cells surrounding the guard cells (Sack & Chen, 2009; Raissig *et al.*, 2016). Nonetheless, although *P. dactylifera* guard cells are equipped with a set of lateral and polar subsidiary cells, grasses have only a lateral pair. In addition to learning about the molecular principles behind the cell–cell interactions within the stomatal complexes of monocots in particular, much can be learned about wax biosynthesis in subsidiary cells that, in date palm, form a chimney around the guard cell pairs. This waxy structure increases the boundary layer resistance, thereby reducing stomatal transpiration.

Subsidiary cells are specialized at providing the guard cells with ions during stomatal opening and sequestering these solutes during stomatal closure (Raschke & Fellows, 1971). This kind of shuttle transport between two cell types requires polar localization of carrier proteins. To draw a complete picture of the unique biology of guard cells and subsidiary cells, their gene expression profiles need to be analysed. The central question is whether these two cell types operate a distinct set of ion channels, carriers and pumps, or whether they use the same transport systems, regulated differentially. By isolating guard cells and subsidiary cells from maize, Buchsenschutz *et al.* (2005) showed that Shaker-type K^+ channels are differentially expressed among the interacting cell pairs. What are the roles of SLAC1 and the ABA signalling pathway in these key anion channels? Interestingly, *Phoenix* stomata respond to ABA fed via the petiole (extra guard cell source) very slowly and incompletely (Fig. 4b). Only when ABA is fed in combination with nitrate is stomatal closure markedly accelerated and enhanced (Fig. 7a). This points towards a role for nitrate as a signalling molecule, which serves as a ligand for efficient stomatal closure and might also link the nitrogen status of the plant with the performance of its stomatal complexes.

We have shown that extracellular nitrate is required to gate open PdSLAC1. Does nitrate regulate the chloride permeability of the *Phoenix* anion channel? If this were the case, one would expect that (1) PdSLAC1 would not be expressed in subsidiary cells, and/or (2) the SLAC1 isoform of subsidiary cells would be inversely nitrate regulated to the S-type anion channel of the guard cell.

Nitrate biology of guard cells

The ability to transport nitrate is associated with numerous anion channel types in living organisms (Fahlke, 2000; Zivic *et al.*, 2009). We have documented that the nitrate/chloride permeability ratio of 20 of *Phoenix* PdSLAC1 is increased relative to *Arabidopsis* AtSLAC1, but is similar to SLAH3 of the model dicot. The *Arabidopsis* SLAC1 has an NO_3^-/Cl^- permeability of 10 and, in SLAH3, it is 20 (Geiger *et al.*, 2009, 2011). Among the taxa, SLAH2 represents the only strictly nitrate-selective channel (Maierhofer *et al.*, 2014b). Plants assimilate carbon CO_2 and nitrogen NO_3^- and synthesize amino acids and other important nitrogen-rich carbon compounds from these building blocks.

Nitrate availability and uptake by guard cells appear to affect stomatal movement in *Arabidopsis* (Guo *et al.*, 2003). In the monocotyledons *Phoenix* palm and rice, the SLAC1 nitrate to chloride permeability is increased relative to the dicotyledonous AtSLAC1 (Fig. S4; Geiger *et al.*, 2009; Sun *et al.*, 2016). This raises the question as to whether monocots, with their guard cells in association with pairs of subsidiary cells, use NO_3^- as a counter anion to K^+ to osmotically drive stomatal movements. If so, does NO_3^-, like K^+, shuttle between guard cells and subsidiary cells? However, because of technical limitations, nitrate levels in open and closed stomata have not yet been quantified. In maize, a monocot grass, Cl^- and K^+ shuttle between guard cells and subsidiarity cells during stomatal movement (Raschke & Fellows, 1971). Similar to the situation in maize, we show here that, in date palm, massive amounts of chloride are released during stomatal closure (Fig. 7c). Nonetheless, this does not exclude the possibility that nitrate could also represent a guard cell anionic osmoticum, but at least in maize and date palms, chloride does represent a major counter anion to potassium.

Acknowledgements

We thank Tracey A. Cuin (University of Tasmania) for critical reading of the manuscript. A.H.A., D.G., E.N., K.A.S.A-R., R.H. and S.A.A. were supported by the King Abdullah Institute for Nanotechnology (KAINS), King Saud University, Riyadh, Saudi Arabia (Award Number N36-15-2). D.G., K.A.S.A-R. and R.H. were supported by grants from the King Saud University, Riyadh, Saudi Arabia. A.B. was supported by a PhD scholarship from Capes Foundation, Ministry of Education of Brazil. R.H. and M.R. were supported by the National Plan for Science, Technology and Innovation (MAARIFAH), King Abdulaziz City for Science and Technology, Saudi Arabia (Award Number 12-ENV2564-02).

Author contributions

P.A., S.A.A., A.B., H.B., D.G., S.L., H.M.M., T.N. and N.S. performed the research and analysed the data. A.H.A., P.A., K.A.S.A-R., J.F., D.G., R.H., K.M. and M.R. designed the study. P.A., K.A.S.A-R., D.G., R.H., H.M.M., K.M. and E.N. wrote the manuscript.

References

Ache P, Bauer H, Kollist H, Al-Rasheid KAS, Lautner S, Hartung W, Hedrich R. 2010. Stomatal action directly feeds back on leaf turgor: new insights into the regulation of the plant water status from non-invasive pressure probe measurements. *Plant Journal* **62**: 1072–1082.

Ache P, Becker D, Ivashikina N, Dietrich P, Roelfsema MR, Hedrich R. 2000. GORK, a delayed outward rectifier expressed in guard cells of *Arabidopsis thaliana*, is a K^+-selective, K^+-sensing ion channel. *FEBS Letters* **486**: 93–98.

Altschul SF, Gish W, Miller W, Myers EW, Lipman DJ. 1990. Basic local alignment search tool. *Journal of Molecular Biology* **215**: 403–410.

Arab L, Kreuzwieser J, Kruse J, Zimmer I, Ache P, Alfarraj S, Al-Rasheid KAS, Schnitzler JP, Hedrich R, Rennenberg H. 2016. Acclimation to heat and drought—lessons to learn from the date palm (*Phoenix dactylifera*). *Environmental and Experimental Botany* **125**: 20–30.

Arabidopsis Genome Initiative. 2000. Analysis of the genome sequence of the flowering plant *Arabidopsis thaliana*. *Nature* **408**: 796–815.

Barthlott W, Neinhuis C, Cutler D, Ditsch F, Meusel I, Theisen I, Wilhelmi H. 1998. Classification and terminology of plant epicuticular waxes. *Botanical Journal of the Linnean Society* **126**: 237–260.

Bauer H, Ache P, Lautner S, Fromm J, Hartung W, Al-Rasheid KA, Sonnewald S, Sonnewald U, Kneitz S, Lachmann N *et al.* 2013. The stomatal response to reduced relative humidity requires guard cell-autonomous ABA synthesis. *Current Biology* **23**: 53–57.

Becker D, Dreyer I, Hoth S, Reid JD, Busch H, Lehnen M, Palme K, Hedrich R. 1996. Changes in voltage activation, Cs^+ sensitivity, and ion permeability in H5 mutants of the plant K^+ channel KAT1. *Proceedings of the National Academy of Sciences, USA* **93**: 8123–8128.

Bemm F, Becker D, Larisch C, Kreuzer I, Escalante-Perez M, Schulze WX, Ankenbrand M, Van de Weyer AL, Krol E, Al-Rasheid KA *et al.* 2016. Venus flytrap carnivorous lifestyle builds on herbivore defense strategies. *Genome Research* **26**: 812–825.

Buchsenschutz K, Marten I, Becker D, Philippar K, Ache P, Hedrich R. 2005. Differential expression of K^+ channels between guard cells and subsidiary cells within the maize stomatal complex. *Planta* **222**: 968–976.

Caine RS, Chater CC, Kamisugi Y, Cuming AC, Beerling DJ, Gray JE, Fleming AJ. 2016. An ancestral stomatal patterning module revealed in the non-vascular land plant *Physcomitrella patens*. *Development* **143**: 3306–3314.

Cardenas-Navarro R, Adamowicz S, Robin P. 1999. Nitrate accumulation in plants: a role for water. *Journal of Experimental Botany* **50**: 613–624.

Chater C, Peng K, Movahedi M, Dunn JA, Walker HJ, Liang YK, McLachlan DH, Casson S, Isner JC, Wilson I *et al.* 2015. Elevated CO_2-induced responses in stomata require ABA and ABA signaling. *Current Biology* **25**: 2709–2716.

Cubero-Font P, Maierhofer T, Jaslan J, Rosales MA, Espartero J, Diaz-Rueda P, Muller HM, Hurter AL, Al-Rasheid KA, Marten I *et al.* 2016. Silent S-type anion channel subunit SLAH1 gates SLAH3 open for chloride root-to-shoot translocation. *Current Biology* **26**: 2213–2220.

De Angeli A, Monachello D, Ephritikhine G, Frachisse JM, Thomine S, Gambale F, Barbier-Brygoo H. 2006. The nitrate/proton antiporter AtCLCa mediates nitrate accumulation in plant vacuoles. *Nature* **442**: 939–942.

Desikan R, Griffiths R, Hancock J, Neill S. 2002. A new role for an old enzyme: nitrate reductase-mediated nitric oxide generation is required for abscisic acid-induced stomatal closure in *Arabidopsis thaliana*. *Proceedings of the National Academy of Sciences, USA* **99**: 16314–16318.

Dragota S, Riederer M. 2007. Epicuticular wax crystals of *Wollemia nobilis*: morphology and chemical composition. *Annals of Botany* **100**: 225–231.

Engineer CB, Hashimoto-Sugimoto M, Negi J, Israelsson-Nordstrom M, Azoulay-Shemer T, Rappel WJ, Iba K, Schroeder JI. 2016. CO_2 sensing and CO_2 peculation of stomatal conductance: advances and open questions. *Trends in Plant Science* **21**: 16–30.

Fahlke C. 2000. Molecular mechanisms of ion conduction in ClC-type chloride channels: lessons from disease-causing mutations. *Kidney International* **57**: 780–786.

Fujii H, Chinnusamy V, Rodrigues A, Rubio S, Antoni R, Park S-Y, Cutler SR, Sheen J, Rodriguez PL, Zhu J-K. 2009. *In vitro* reconstitution of an ABA signaling pathway. *Nature* **462**: 660–664.

Geiger D, Maierhofer T, Al-Rasheid KA, Scherzer S, Mumm P, Liese A, Ache P, Wellmann C, Marten I, Grill E *et al.* 2011. Stomatal closure by fast abscisic acid signaling is mediated by the guard cell anion channel SLAH3 and the receptor RCAR1. *Science Signalling* **4**: ra32.

Geiger D, Scherzer S, Mumm P, Stange A, Marten I, Bauer H, Ache P, Matschi S, Liese A, Al-Rasheid KA *et al.* 2009. Activity of guard cell anion channel SLAC1 is controlled by drought-stress signaling kinase-phosphatase pair. *Proceedings of the National Academy of Sciences, USA* **106**: 21425–21430.

Guo FQ, Young J, Crawford NM. 2003. The nitrate transporter AtNRT1.1 (CHL1) functions in stomatal opening and contributes to drought susceptibility in *Arabidopsis*. *Plant Cell* **15**: 107–117.

Guzel Deger A, Scherzer S, Nuhkat M, Kedzierska J, Kollist H, Brosche M, Unyayar S, Boudsocq M, Hedrich R, Roelfsema MR. 2015. Guard cell SLAC1-type anion channels mediate flagellin-induced stomatal closure. *New Phytologist* **208**: 162–173.

Hashimoto M, Negi J, Young J, Israelsson M, Schroeder JI, Iba K. 2006. *Arabidopsis* HT1 kinase controls stomatal movements in response to CO_2. *Nature Cell Biology* **8**: 391–397.

Hedrich R. 2012. Ion channels in plants. *Physiological Reviews* **92**: 1777–1811.

Hetherington AM, Woodward FI. 2003. The role of stomata in sensing and driving environmental change. *Nature* **424**: 901–908.

Holloway PJ. 1982. Structure and histochemistry of plant cuticular membranes: an overview. In: Cutler DF, Alvin KL, Price CE, eds. *The plant cuticle*. London, UK: Academic Press, 1–32.

Hu H, Boisson-Dernier A, Israelsson-Nordstrom M, Bohmer M, Xue S, Ries A, Godoski J, Kuhn JM, Schroeder JI. 2010. Carbonic anhydrases are upstream regulators of CO_2-controlled stomatal movements in guard cells. *Nature Cell Biology* **12**: 87–93.

Hua D, Wang C, He J, Liao H, Duan Y, Zhu Z, Guo Y, Chen Z, Gong Z. 2012. A plasma membrane receptor kinase, GHR1, mediates abscisic acid- and hydrogen peroxide-regulated stomatal movement in Arabidopsis. *Plant Cell* **24**: 2546–2561.

Humble GD, Raschke K. 1971. Stomatal opening quantitatively related to potassium transport: evidence from electron probe analysis. *Plant Physiology* **48**: 447–453.

Koers S, Guzel-Deger A, Marten I, Roelfsema MR. 2011. Barley mildew and its elicitor chitosan promote closed stomata by stimulating guard-cell S-type anion channels. *Plant Journal* **68**: 670–680.

Kusumi K, Hirotsuka S, Kumamaru T, Iba K. 2012. Increased leaf photosynthesis caused by elevated stomatal conductance in a rice mutant deficient in SLAC1, a guard cell anion channel protein. *Journal of Experimental Botany* **63**: 5635–5644.

Langer K, Levchenko V, Fromm J, Geiger D, Steinmeyer R, Lautner S, Ache P, Hedrich R. 2004. The poplar K^+ channel KPT1 is associated with K^+ uptake during stomatal opening and bud development. *Plant Journal* **37**: 828–838.

Lee SC, Lan W, Buchanan BB, Luan S. 2009. A protein kinase-phosphatase pair interacts with anion channel to regulate ABA signaling in plant guard cells. *Proceedings of the National Academy of Sciences, USA* **106**: 21419–21424.

Levchenko V, Konrad KR, Dietrich P, Roelfsema MR, Hedrich R. 2005. Cytosolic abscisic acid activates guard cell anion channels without preceding Ca^{2+} signals. *Proceedings of the National Academy of Sciences, USA* **102**: 4203–4208.

Luis ZG, Bezerra KMG, Scherwinski-Pereira JE. 2010. Adaptability and leaf anatomical features in oil palm seedlings produced by embryo rescue and pre-germinated seeds. *Brazilian Journal of Plant Physiology* **22**: 209–215.

Ma Y, Szostkiewicz I, Korte A, Moes D, Yang Y, Christmann A, Grill E. 2009. Regulators of PP2C phosphatase activity function as abscisic acid sensors. *Science* **324**: 1064–1068.

Maierhofer T, Diekmann M, Offenborn JN, Lind C, Bauer H, Hashimoto K, Al-Rasheid KAS, Luan S, Kudla J, Geiger D *et al.* 2014a. Site- and kinase-specific phosphorylation-mediated activation of SLAC1, a guard cell anion channel stimulated by abscisic acid. *Science Signalling* **7**: ra86.

Maierhofer T, Lind C, Huttl S, Scherzer S, Papenfuss M, Simon J, Al-Rasheid KA, Ache P, Rennenberg H, Hedrich R *et al.* 2014b. A single-pore residue renders the *Arabidopsis* root anion channel SLAH2 highly nitrate selective. *Plant Cell* **26**: 2554–2567.

Marten H, Hedrich R, Roelfsema MR. 2007. Blue light inhibits guard cell plasma membrane anion channels in a phototropin-dependent manner. *Plant Journal* **50**: 29–39.

Martinoia E, Heck U, Wiemken A. 1981. Vacuoles as storage compartments for nitrate in barley leaves. *Nature* **289**: 292–294.

Meyer S, Mumm P, Imes D, Endler A, Weder B, Al-Rasheid KA, Geiger D, Marten I, Martinoia E, Hedrich R. 2010. AtALMT12 represents an R-type anion channel required for stomatal movement in *Arabidopsis* guard cells. *Plant Journal* **63**: 1054–1062.

Negi J, Matsuda O, Nagasawa T, Oba Y, Takahashi H, Kawai-Yamada M, Uchimiya H, Hashimoto M, Iba K. 2008. CO_2 regulator SLAC1 and its homologues are essential for anion homeostasis in plant cells. *Nature* **452**: 483–486.

Nour-Eldin HH, Hansen BG, Norholm MH, Jensen JK, Halkier BA. 2006. Advancing uracil-excision based cloning towards an ideal technique for cloning PCR fragments. *Nucleic Acids Research* **34**: e122.

Park SY, Fung P, Nishimura N, Jensen DR, Fujii H, Zhao Y, Lumba S, Santiago J, Rodrigues A, Chow TF *et al.* 2009. Abscisic acid inhibits type 2C protein phosphatases via the PYR/PYL family of START proteins. *Science* **324**: 1068–1071.

Raissig MT, Abrash E, Bettadapur A, Vogel JP, Bergmann DC. 2016. Grasses use an alternatively wired bHLH transcription factor network to establish stomatal identity. *Proceedings of the National Academy of Sciences, USA* **113**: 8326–8331.

Raschke K, Fellows MP. 1971. Stomatal movement in *Zea mays*: shuttle of potassium and chloride between guard cells and subsidiary cells. *Planta* **101**: 296–316.

Reynolds ES. 1963. The use of lead citrate at high pH as an electron opaque stain in electron microscopy. *Journal of Cell Biology* **17**: 208–212.

Roelfsema MR, Hanstein S, Felle HH, Hedrich R. 2002. CO_2 provides an intermediate link in the red light response of guard cells. *Plant Journal* **32**: 65–75.

Roelfsema MR, Hedrich R. 2005. In the light of stomatal opening: new insights into 'the Watergate'. *New Phytologist* **167**: 665–691.

Roelfsema MR, Hedrich R, Geiger D. 2012. Anion channels: master switches of stress responses. *Trends in Plant Science* **17**: 221–229.

Roelfsema MR, Steinmeyer R, Staal M, Hedrich R. 2001. Single guard cell recordings in intact plants: light-induced hyperpolarization of the plasma membrane. *Plant Journal* **26**: 1–13.

Sack FD, Chen JG. 2009. Plant science. Pores in place. *Science* **323**: 592–593.

Schroeder JI, Hagiwara S. 1990. Repetitive increases in cytosolic Ca^{2+} of guard cells by abscisic acid activation of nonselective Ca^{2+} permeable channels. *Proceedings of the National Academy of Sciences, USA* **87**: 9305–9309.

Schuster AC, Burghardt M, Alfarhan A, Bueno A, Hedrich R, Leide J, Thomas J, Riederer M. 2016. Effectiveness of cuticular transpiration barriers in a desert plant at controlling water loss at high temperatures. *AoB Plants* **8**: plw027.

Soon FF, Ng LM, Zhou XE, West GM, Kovach A, Tan MH, Suino-Powell KM, He Y, Xu Y, Chalmers MJ, *et al.* 2012. Molecular mimicry regulates ABA signaling by SnRK2 kinases and PP2C phosphatases. *Science* **335**: 85–88.

Speer M, Kaiser WM. 1991. Ion relations of symplastic and apoplastic space in leaves from *Spinacia oleracea* L. and *Pisum sativum* L. under salinity. *Plant Physiology* **97**: 990–997.

Spurr AR. 1964. A low viscosity epoxy resin embedding medium for electron microscopy. *Journal of Ultrastructure Research* **26**: 31–43.

Stebbins GL, Khush GS. 1961. Variation in the organization of the stomatal complex in the leaf epidermis of monocotyledons and its bearing on their phylogeny. *American Journal of Botany* **48**: 51–59.

Sun SJ, Qi GN, Gao QF, Wang HQ, Yao FY, Hussain J, Wang YF. 2016. Protein kinase OsSAPK8 functions as an essential activator of S-type anion channel OsSLAC1, which is nitrate-selective in rice. *Planta* **243**: 489–500.

Tian W, Hou C, Ren Z, Pan Y, Jia J, Zhang H, Bai F, Zhang P, Zhu H, He Y *et al.* 2015. A molecular pathway for CO_2 response in *Arabidopsis* guard cells. *Nature Communications* **6**: 6057.

Trapnell C, Roberts A, Goff L, Pertea G, Kim D, Kelley DR, Pimentel H, Salzberg SL, Rinn JL, Pachter L. 2012. Differential gene and transcript expression analysis of RNA-seq experiments with TopHat and Cufflinks. *Nature Protocols* **7**: 562–578.

Vahisalu T, Kollist H, Wang YF, Nishimura N, Chan WY, Valerio G, Lamminmaki A, Brosche M, Moldau H, Desikan R *et al.* 2008. SLAC1 is required for plant guard cell S-type anion channel function in stomatal signalling. *Nature* **452**: 487–491.

Yamauchi S, Takemiya A, Sakamoto T, Kurata T, Tsutsumi T, Kinoshita T, Shimazaki K. 2016. The plasma membrane H^+-ATPase AHA1 plays a major role in stomatal opening in response to blue light. *Plant Physiology* **171**: 2731–2743.

Zabka V, Stangl M, Bringmann G, Vogg G, Riederer M, Hildebrandt U. 2008. Host surface properties affect prepenetration processes in the barley powdery mildew fungus. *New Phytologist* **177**: 251–263.

Zivic M, Popovic M, Todorovic N, Vucinic Z. 2009. Outwardly rectifying anionic channel from the plasma membrane of the fungus *Phycomyces blakesleeanus*. *Eukaryotic Cell* **8**: 1439–1448.

Supporting Information

Additional Supporting Information may be found online in the Supporting Information tab for this article:

Fig. S1 Subsidiary cells are the sites of epicuticular wax production to form chimneys around stomatal complexes.

Fig. S2 Diffusion of solutes in excised date palm leaves is faster than in *Arabidopsis*.

Fig. S3 Phylogenetic analysis of PdSLAC1 and PdOST1 using the online tool 'One Click' at http://www.phylogeny.fr/ with default settings.

Fig. S4 PdSLAC1 is 20 times more permeable for nitrate than for chloride.

Fig. S5 KCl does not influence stomatal performance of date palms.

Table S1 RNAseq data: abscisic acid (ABA) treatment affects 153 date palm genes

Please note: Wiley Blackwell are not responsible for the content or functionality of any Supporting Information supplied by the authors. Any queries (other than missing material) should be directed to the *New Phytologist* Central Office.